

Atrial Electromechanical Cycle Length Mapping in Paced Canine Hearts *In Vivo*

Alexandre Costet, Ethan Bunting, Julien Grondin, Alok Gambhir, and Elisa E. Konofagou

Abstract—Atrial arrhythmias affect millions of people worldwide. Characterization and study of arrhythmias in the atria in the clinic is currently performed point by point using mapping catheters capable of generating maps of the electrical activation rate or cycle length. In this paper, we describe a new ultrasound-based mapping technique called electromechanical cycle length mapping (ECLM) capable of estimating the electromechanical activation rate, or cycle length, i.e., the rate of the mechanical activation of the myocardium which follows the electrical activation. ECLM relies on frequency analysis of the incremental strain within the atria and can be performed in a single acquisition. ECLM was validated in a canine model paced from the left atrial appendage, against pacing rates within the reported range of cycle lengths previously measured during atrial arrhythmias such as atrial fibrillation. Correlation between the global estimated electromechanical cycle lengths and pacing rates was shown to be excellent (slope = 0.983, intercept = 3.91, $r^2 = 0.9999$). The effect of the number of cardiac cycles on the performance of ECLM was also investigated and the reproducibility of ECLM was demonstrated (error between consecutive acquisitions for all pacing rates: $6.3 \pm 4.3\%$). These findings indicate the potential of ECLM for noninvasively characterizing atrial arrhythmias and provide feedback on the treatment planning of catheter ablation procedures in the clinic.

I. INTRODUCTION

ATRIAL arrhythmias such as atrial fibrillation (AF) affect millions of people worldwide. Over 2 million people are diagnosed with AF in North America, whereas in Europe, this number is over 4 million [1]. Although not fatal, atrial arrhythmias, and AF in particular, affect the quality of life of patients due to a range of symptoms including shortness of breath, chest pains, fatigue, palpitations, lightheadedness, or even syncope [2]. Additionally, serious complications can occur and lead to stroke, and more rarely, sudden cardiac death [3], [4]. Atrial arrhythmias can be managed by antiarrhythmic drugs, direct current cardioversion, and catheter ablation [5].

Over the past decade, catheter ablation procedures, especially in the case of AF, have become more common in

many hospital and cardiac centers around the world [6]. During such procedures, a map of the activation rate, or cycle length (CL), is usually acquired before proceeding to ablation. Those activation maps reflect the underlying electrical activation of the heart and remain the gold standard when it comes to arrhythmia characterization because they enable clinicians to detect regions most likely responsible for sustaining the arrhythmia [5].

The CL parameter is obtained by recording intra-cardiac electrical signals or electrograms (EGM) using an electrode-tipped catheter at various points within the heart. Catheters for mapping usually carry one to ten electrodes, which are arranged either linearly [7], in a circle [8], or as an array [9]. Despite the numerous electrodes, mapping requires point-by-point acquisition to map the entire atria. Non-contact mapping catheters with 64 electrodes are also used in the clinic and rely on solving an inverse problem to reconstruct the electrical signals coming from the myocardium [10]. Study of the CL parameter has given clinicians and researchers insights into the mechanisms maintaining AF such as atrial remodeling, re-entry circuits, the existence of a left-to-right gradient of the electrical activation rate, and drivers of AF such as rotors [11]–[15]. Concurrently, dominant frequency (DF) analysis for the study of EGMs was introduced [9], [13], [16]–[19]. By analyzing the frequency spectra of the EGMs acquired, it is possible to determine for each mapping location the DF of the signal. It has been shown that the DF is inversely proportional to the activation rate, or CL [20]. Studies showed that regions of highest DF, i.e., shorter CL, were found to be mainly localized in the left atrium (LA) during AF [12]. Similarly to CL, a DF gradient was observed in the atria [11], [13], [17], [21] and ablations at the site of highest DFs were shown to result in the slowing or termination of AF [13]. This led to the belief that regions of high DF and fractionated EGM may perpetuate AF [19]. Typical values of CL and DF for atrial arrhythmias have been reported to range from 100 to 250 ms or 4 to 10 Hz, respectively [18], [22].

Electromechanical cycle length mapping (ECLM) is a new ultrasound-based mapping technique similar to electromechanical wave imaging (EWI) [23]–[26]. ECLM relies on the noninvasive transmural estimation of the incremental strain, i.e., the inter-frame strain, in the myocardium at high temporal and spatial resolution. However, unlike EWI, which tracks the propagation of the electromechanical wave, i.e., the wave of transient deformations occurring in response to local electrical activation, ECLM entails the study of the frequency component of the incremental strain, and by extension, the frequency and rate of activa-

Manuscript received December 11, 2014; accepted April 18, 2015. This study was supported in part by the National Institutes of Health (R01 EB006042 and R01 HL114358).

A. Costet, E. Bunting, J. Grondin, and E. E. Konofagou are with the Department of Biomedical Engineering, Columbia University, New York, NY, 10027, USA (e-mail: ek2191@columbia.edu).

A. Gambhir is with the Department of Medicine–Cardiology, Columbia University, New York, NY, 10032, USA.

E. E. Konofagou is also with the Department of Radiology, Columbia University, New York, NY, 10032, USA.

DOI <http://dx.doi.org/10.1109/TUFFC.2014.006932>

TABLE I. SUMMARY OF PACING RATES AND NUMBER OF CORRESPONDING ACQUISITIONS.

Pacing rates (ms)	150	170	200	250	300	350	400	500
Number of acquisitions	2	1	5	4	3	1	1	1

tion without the need to select an origin of activation as is the case for EWI. Thus, ECLM was developed for the characterization of nonperiodic arrhythmias such as AF where choosing an origin of activation does not apply.

The goal of this study was to develop and validate a new mapping method, ECLM, to map the electromechanical activation rate of the entire atrium in a single acquisition. To achieve the aforementioned goals, an atrial tachycardia canine model was generated by pacing the heart from the left atrial appendage at a rate within the range reported during AF [18], [22]. Maps and histograms of the CL during pacing were compared with the known pacing rate, and the correlation between the paced and detected rate was computed. Next, we evaluated the effect of the length of acquisition on the ECLM quality by comparing results obtained from 1-s, 2-s, and 4-s-long acquisitions. Finally, reproducibility was assessed by comparing maps and histograms from two consecutive acquisitions.

II. METHODS

A. Experimental Protocol

This study conformed to the Public Health Service Policy on Humane Care and Use of Laboratory Animals and was approved by the Institutional Animal Care and Use Committee of Columbia University. Six normal male adult mongrel canines weighting 24.1 ± 0.4 kg were used in this study. Canines were anesthetized with an intravenous injection of diazepam ($0.5\text{--}1.0$ mg·kg⁻¹) or an intramuscular injection of hydromorphone (0.05 mg·kg⁻¹) as premedication, and methohexital ($4\text{--}11$ mg·kg⁻¹) as induction anesthetic. Anesthesia was maintained by a mixture of oxygen and isoflurane ($0.5\text{--}5.0\%$) delivered through mechanical ventilation via a rate- and volume-regulated ventilator. Morphine (0.15 mg·kg⁻¹, epidural) was administered before surgery, and lidocaine (50 μg·kg⁻¹·h⁻¹, intravenous) was used during the entire procedure. To maintain blood volume, a 0.9% saline solution was administered intravenously at 5 mL·kg⁻¹·h⁻¹. Oxygen, peripheral blood pressure, and temperature were monitored throughout the experiment. Standard limb leads were placed for surface electrocardiogram (ECG) monitoring. The chest was opened by lateral thoracotomy using electrocautery. A pacing electrode was sutured to the left atrial appendage (LAA). Pacing rates were chosen to be within AF and atrial flutter range and ranged from 150 to 500 ms (see Table I). Data acquisition was performed on free-breathing, open-chest canines during pacing from the LAA, which was confirmed by monitoring of the ECG. Data were acquired during a total of 18 different experimental setups, or pacing schemes, as detailed in Table I.

B. Electromechanical Cycle Length Mapping

ECLM was performed in the four-chamber, two-chamber, long-axis, and 3.5-chamber echocardiographic apical views during pacing from the LAA. The apical 3.5-chamber view corresponds to an apical view taken in between the four- and two-chamber views. Similar to EWI [24]–[26], ECLM relies on RF-based motion estimation [27] and gradient operators [28] to map the transient deformations (or strains) occurring during electrical activation of the myocardium. A minimum frame rate is required for precise estimation of displacement and cardiac strain [25], [29]. In a previous study [25], our group has shown that when estimating incremental strain in EWI, the framerate has to be sufficiently high, i.e., inter-frame time sufficiently short, to prevent decorrelation at higher strains due to 3-D motion, but not too high so as to prevent estimation ambiguity from random noise at very low strains. Our group has reported that a framerate between 500 and 2000 Hz guarantees the highest SNR possible for the incremental strain estimation [25]. An unfocused transmit sequence [30] was developed and used on a Verasonics system (Verasonics, Redmond, WA, USA) to acquire RF frames at 2000 fps (Fig. 1.1) using a 2.5-MHz ATL P4-2 phased array. Such a high frame rate can be achieved by emitting unfocused, spherical ultrasound waves using a virtual focus located 10.2 mm behind the array as described in a previous study from our group [31]. Beamforming on the raw signals obtained from each of the elements, i.e., signals acquired by each of the element without any processing or filtering, was performed during postprocessing, resulting in the reconstruction of one RF frame per transmit. Because the B-mode images reconstructed from these unfocused transmit sequences have lower resolution and SNR, thus rendering segmentation difficult, a standard 64-line B-mode acquisition was performed following the initial high frame rate acquisition. The complete acquisition sequence thus consisted of 2 s or 4 s of high frame rate acquisition at 2000 fps (4000 or 8000 frames acquired), followed by an anatomical imaging sequence consisting of 1.5 s of a standard 64-line B-mode acquisition at 30 fps (Fig. 1.1). The 2-s and 4-s lengths of acquisition were chosen according to heart rate and/or pacing rate to acquire enough data to span at least a couple of cardiac cycles. Retrospective ECG-gating was used to temporally align the high frame rate acquisition with the anatomical B-mode acquisition, but not for motion estimation unlike previous approaches [24].

RF frames were reconstructed in polar coordinates from the raw signals obtained from the probe elements using a delay-and-sum algorithm as described elsewhere [31]. The reconstructed images had an angular sampling of 0.7° or 0.025 rad (128 lines spanning 90°) and an axial sampling

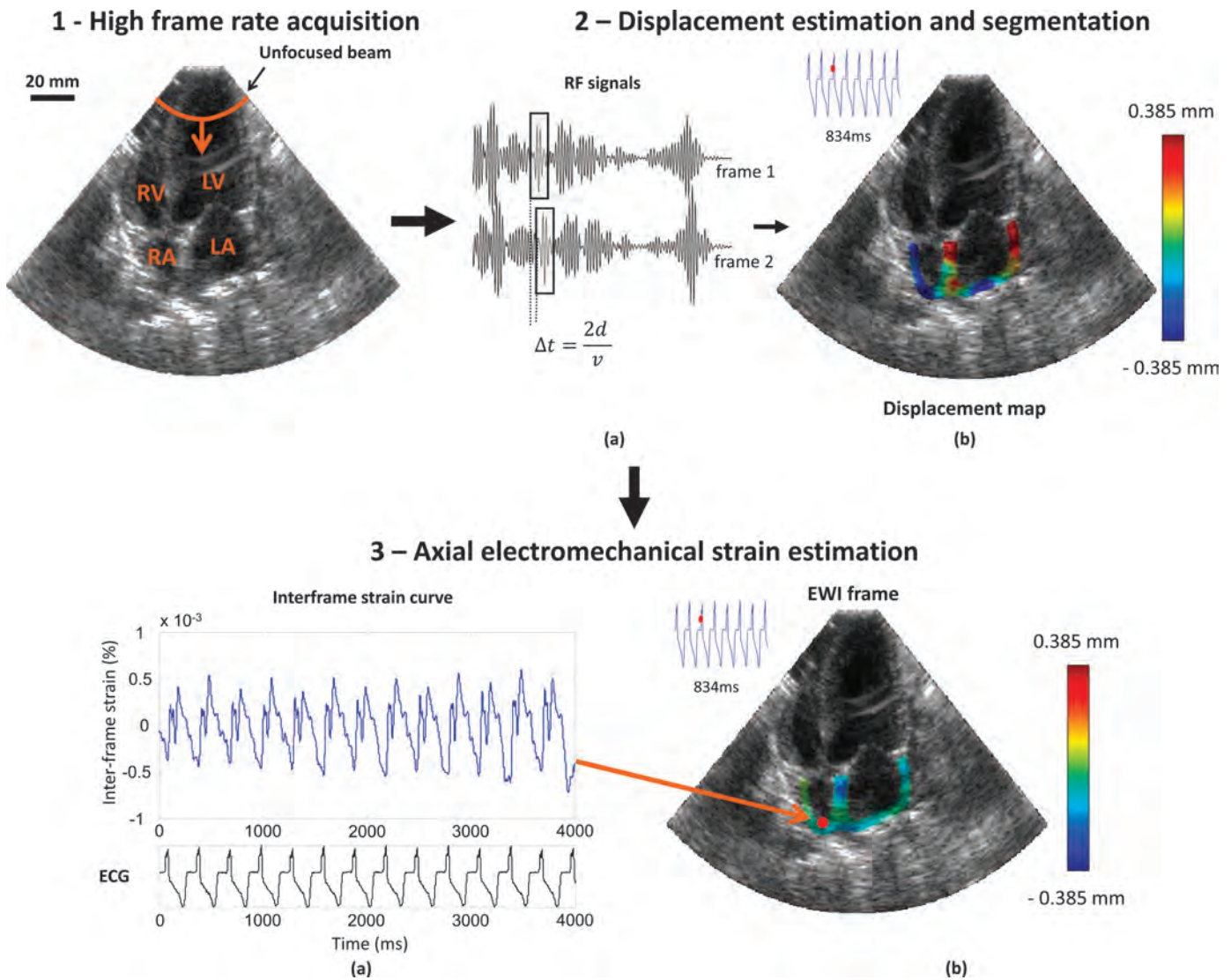


Fig. 1. Data acquisition and motion and strain estimation flowchart: (1) 2-s or 4-s high frame-rate acquisition (2000 Hz) of standard apical RF images with an unfocused transmit sequence. (2) Longitudinal displacement estimation is performed using 1-D cross-correlation (a), and motion maps are generated (b). (3) Axial incremental strains are estimated using a least-square estimator (a) and are overlaid onto the B-mode images to produce videos (b). RA: right atrium, LA: left atrium, RV: right ventricle, LV: left ventricle.

frequency of 20 MHz (axial sampling of 0.0385 mm) [30]. Segmentation of the myocardium was manually initialized on the first frame of the anatomical B-mode sequence, and the endocardial contour was subsequently automatically tracked throughout the cardiac cycle using the estimated displacements [32]. Displacement estimation was performed using a fast, 1-D cross-correlation algorithm [27] with overlapping 9.2-mm axial windows (15 wavelengths) and a 0.385 mm window shift corresponding to a 96% overlap (Fig. 1.2). Previous studies by our group and others have shown that a window size within the range of 10 to 15 wavelengths produced the optimal results for motion estimation [33], [34]. Indeed, a large window size improves the SNR and reduces jitter errors of motion estimation [35]–[37], whereas too large of a window may include larger intra-window deformation and in turn affect the spatial resolution of motion estimation [38]. Spatial resolution for motion estimation is determined by the win-

dow shift (or overlap), which here is 0.385 mm and was chosen according to previous studies so as to maximize the resolution for optimal estimation [30], [34], [38]. Axial incremental strains (i.e., the inter-frame strain in the axial direction) were estimated using a least-square estimator with a 5-mm, 1-D-kernel (Fig. 1.3) [28]. Strain estimates were then filtered using a 12 mm by 10 beams moving average spatial filter and a temporal low-pass filter with a 125-Hz cutoff frequency. The displacement and strain estimation was performed in polar coordinates. Displacements and strains were subsequently converted to Cartesian coordinates.

Our CL parameter is similar to the CL parameter used in the electrophysiology suite, which is determined during ablation procedure except that it measures the electromechanical activation rate rather than the electrical activation rate. To estimate the period of activation in the atria during pacing, i.e., the CL, we obtained the frequency

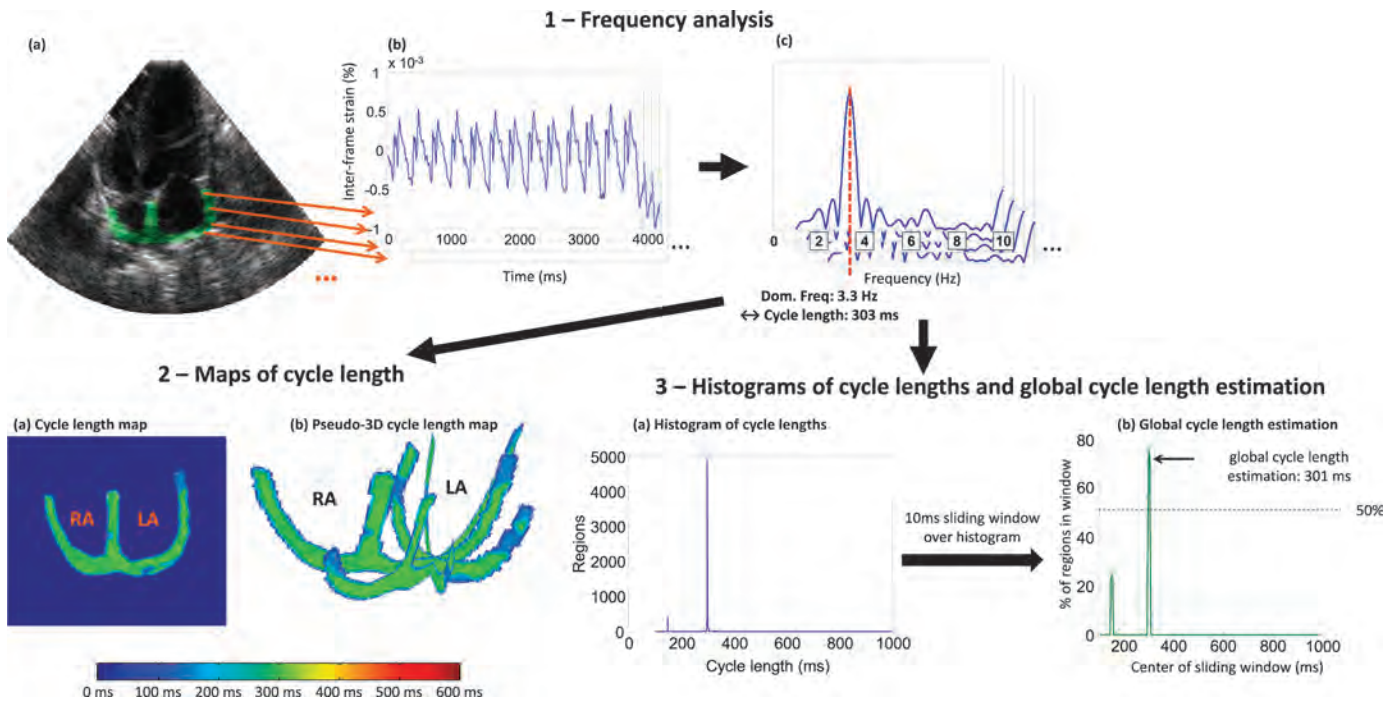


Fig. 2. ECLM flowchart: (1) At each point within the segmented region, the frequency spectrum associated with the corresponding inter-frame strain curves estimated previously is obtained by FFT. Using the frequency spectra, the dominant frequency is extracted and converted to cycle length at each point within the mask. (2) Maps of cycle lengths are generated from the dominant frequencies estimated previously (a). From the cycle length maps obtained in four apical views (4-chamber, 2-chamber, long-axis, 3.5-chamber taken in between the 2- and 4-chamber views), pseudo-3-D maps are generated (b). (3) Histograms of the cycle length in the atria are generated (a). For each acquisition, a 10-ms-wide window is slid over the range of the histogram and the global cycle length of the acquisition is obtained by considering the center of the sliding window containing over 50% of the regions in the atria (b). RA: right atrium, LA: left atrium, RV: right ventricle, LV: left ventricle.

spectra of all points in the atria by applying a fast Fourier transform (FFT) to the previously estimated incremental strain curves. The FFT of an N -point signal yields the N -point discrete Fourier transform with a highest resolvable frequency of $f_s/2$, and with a frequency resolution given by the following equation: $df = f_s/N$ with df the frequency resolution, f_s the sampling frequency of the signal, and N the number of samples acquired. To obtain a frequency resolution of $df = 0.01$ Hz, each strain curve was first resampled to an appropriate frequency following the equation for the FFT frequency resolution. The resampled strain curves were then zero-padded when necessary to match the initial length of the signal acquired before the FFT was applied. Thus, because we applied the FFT to 1-s, 2-s, and 4-s-long signals acquired at 2000 Hz (corresponding to 2000-, 4000-, and 8000-sample-long signals, respectively), the strain curves were resampled to 20, 40, and 80 Hz respectively. This enabled us to detect frequencies ranging from 0 to 10, 20, and 40 Hz respectively. The FFT was applied to the strain curves obtained at each point within the mask of the atria, and from each resulting frequency spectrum we detected the DF and converted that value to CL (Fig. 2.1).

Next, CL maps were generated for each of the four apical views (4-chamber, 2-chamber, 3.5-chamber, and long-axis) by plotting the CL detected at each point within the mask [Fig. 2.2(a)]. From these four maps, pseudo-3-D CL maps were generated for each acquisition [Fig. 2.2(b)]. In

parallel, histograms of the CLs in the atria during pacing were generated for each view and each single-view histogram was included into a single histogram per acquisition at a given pacing rate [Fig. 2.3(a)]. From these histograms, the global CL for each acquisition was detected by sliding a 10-ms-wide window over the range of CLs. The value at the center of the window containing the majority of the regions in the atria was taken as the global CL for the considered acquisition, provided it contained at least 50% of all regions in the atria [Fig. 2.3(b)]. The resulting CL maps and histograms are presented in Fig. 3. Correlation between global CL and pacing rate is presented in Fig. 4.

Comparison between varying lengths of acquisition (Fig. 5) and successive acquisitions (Fig. 6) was achieved by generating maps of the absolute difference of corresponding views between two acquisitions (successive or of varying lengths). Pseudo-3-D difference maps were then generated from these maps. Finally, a quantitative metric of the difference was derived by computing the sum of the absolute difference between ECLM maps from the two different types of acquisitions and expressing that value relative to the average sum of all CL within the mask between the two acquisitions. We call the resulting value the error:

$$\text{error} = \frac{\sum_1^M |f(i) - g(i)|}{\frac{1}{2} \sum_1^M (f(i) + g(i))},$$

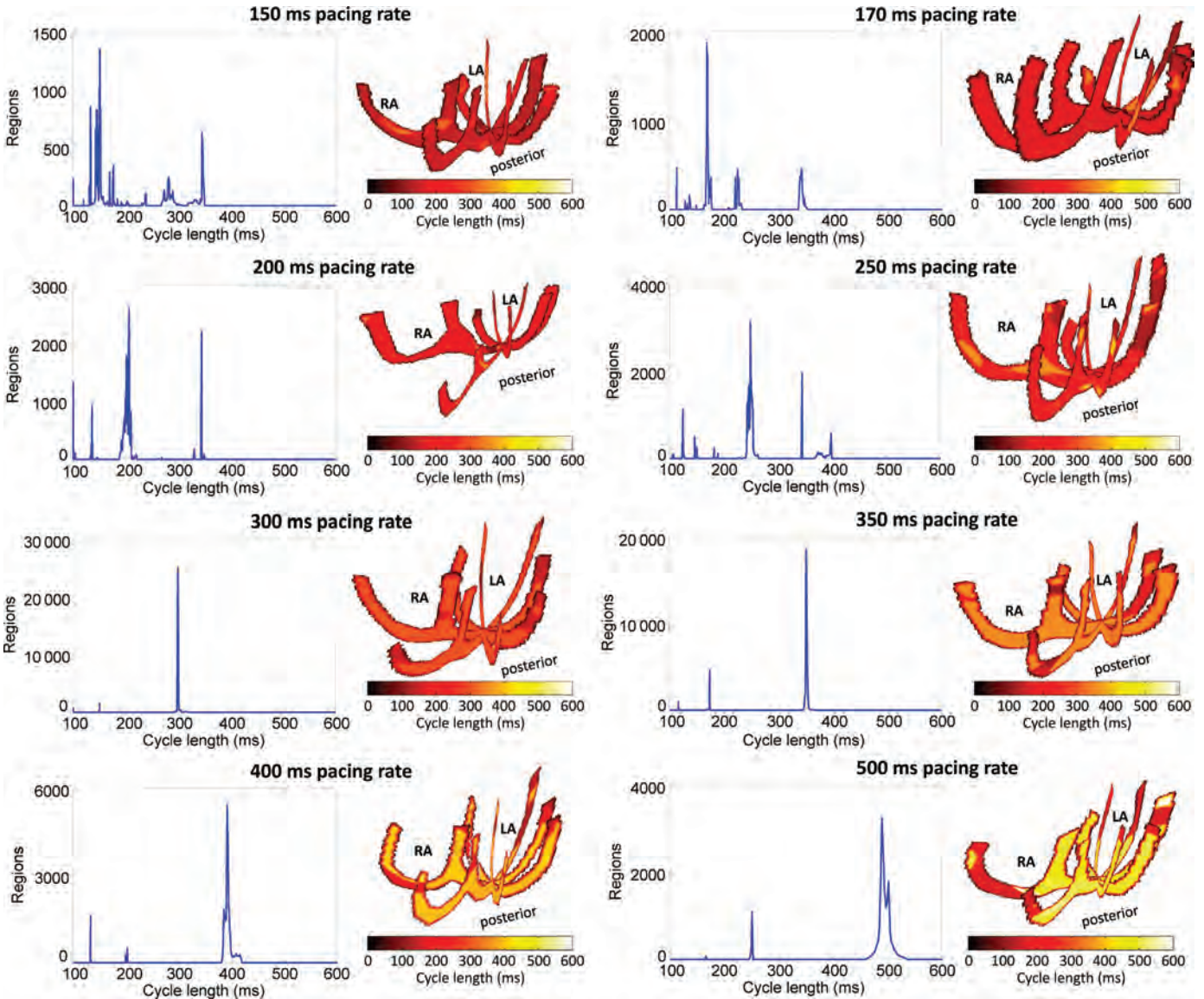


Fig. 3. Histograms and maps of cycle lengths in canines heart *in vivo* during pacing of the left atrial appendage at a pacing rate of 150, 170, 200, 250, 300, 350, 400, and 500 ms. Pseudo-3-D cycle length maps are presented with the posterior side facing front. In each case, the main peak in the histogram corresponds to the pacing rate. Maps confirm that, for each pacing rate, most of the myocardium in the atria is activated at a cycle length corresponding to the pacing rate. RA: right atrium, LA: left atrium.

with f and g the maps of the ECLM-detected CL for the first and second acquisition, respectively, and M the total number of points in the segmented region.

III. RESULTS

A. Histograms and Maps of Cycle Lengths

In Fig. 3, we present histograms and CL maps in canines *in vivo* during pacing from the LAA. The rates of pacing ranged from 150 to 500 ms. Pseudo-3-D CL maps are presented with the posterior side facing front. For each pacing rate, the global maximum on the histogram corresponds to the pacing rate. One can note that as the pacing rate decreases, the global maximum in the histo-

gram becomes clearer: for pacing at 150 through 250 ms, although the global maximum is at the expected rate, we note numerous local maxima located around the pacing rate. CL maps presented next to the corresponding histogram confirm that most of the atria activated at the same CL as the pacing rate. Similar to the histograms, as the pacing rate decreases, the CL maps become more uniform, indicating that a bigger percentage of the atria activates at the pacing rate.

B. Global ECLM-Detected Activation Cycle Length Versus LAA Pacing Rate

Fig. 4 shows a plot of the global ECLM-detected activation cycle length, as described in Section II, versus the LAA pacing rate. The plot was obtained by considering 18

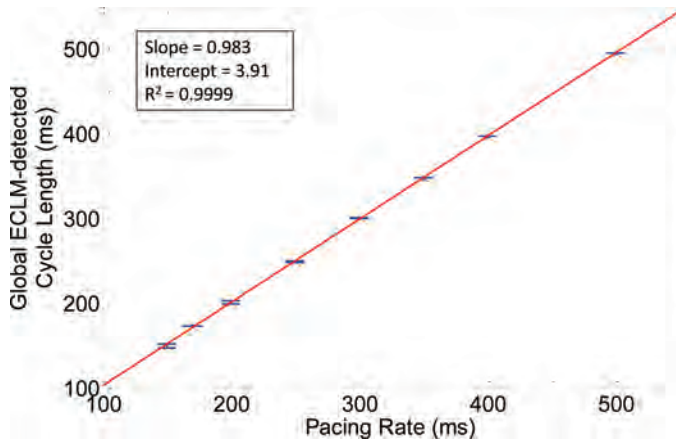


Fig. 4. Global ECLM-detected activation cycle length versus LAA pacing rate.

points, each corresponding to the different pacing schemes as detailed in Table I. For each pacing scheme, the average value and standard deviation of the global ECLM-detected activation CLs were computed from all acquisitions, when applicable. A summary of those values can be found in Table II. An excellent correlation between the ECLM-detected activation CL and the underlying pacing rate was obtained.

C. Effect of Acquisition Length on ECLM

Fig. 5 shows the effect of the length of acquisition on the performance of ECLM. In this study, we examined the difference between 1-s, 2-s, and 4-s-long acquisitions during pacing at 350 ms. Comparison of the corresponding CL maps shows that, qualitatively, all three CL maps are very similar to the point of being almost indistinguishable [Fig. 5(a)]. Absolute difference maps are also presented and show that CL maps only differ in localized areas [Fig. 5(b)]. Quantitatively, the error was 4.3% between 1-s and 2-s-long acquisitions, 2.4% between 1-s and 4-s-long acquisitions, and 1.8% between 2-s and 4-s-long acquisitions.

D. ECLM Reproducibility

In Fig. 6, we demonstrate ECLM reproducibility by comparing ECLM results between two consecutive 2-s-long acquisitions for each of the pacing rates used in this

study. Qualitatively, the majority of the difference maps show that the differences between the two corresponding acquisitions are very small, except in a few localized areas such as near the base in the lateral wall of the LA (350 ms case) or in the septum (170, 300, and 350 ms cases), and at the mid-level in the lateral wall of the RA (200 ms case). A wide region of error can be seen while pacing at 170 ms in the posterior atrial apical region. That region corresponds to an absolute error of 170 ms, which means that for one of the acquisitions ECLM found that the region activated at half the rate expected. Cases corresponding to pacing at 400 and 500 ms both show regions of higher errors than in other pacing case. Additionally, pacing at 500 ms shows a higher number of errors. Quantitatively, the errors between CL maps from consecutive acquisitions are summarized in Table III. Reproducibility error is less than 10% for all cases except pacing at 170 ms, with pacing at 250 and 300 ms showing the least errors. Overall, the average error between consecutive acquisitions is $6.3 \pm 4.3\%$.

IV. DISCUSSION

The goal of this study was to introduce a new mapping method, ECLM, which can map the CL of electromechanical activation of the heart noninvasively. Furthermore, the study aimed at validating ECLM against well-defined and controlled heart rhythms to provide a basis for the study of more complex atrial arrhythmias such as AF or flutter.

ECLM relies on the same principle as EWI, which our group previously reported on, namely the characterization of the electromechanical activation of the heart using motion and strain estimation techniques on RF signals [23]–[26], [30], [31]. The electromechanical activation of the heart follows the electrical activation pattern with a delay of a few milliseconds [39], [40] and corresponds to the initial time point at which the cardiac muscle starts its contraction. EWI is usually conducted over atrial and/or ventricular systole and requires choosing an origin and tracking the electromechanical activation from that moment. However, unlike EWI, ECLM studies the frequency information of the electromechanical activation, i.e., the periodicity at which the heart activates. ECLM is thus aimed at studying arrhythmias such as fibrillation where

TABLE II. SUMMARY OF THE GLOBAL ECLM-DETECTED ACTIVATION RATE FOR EACH PACING SCHEME AND OF THE CORRESPONDING GLOBAL ECLM-DETECTED ACTIVATION CYCLE LENGTHS.

Pacing rate (ms)	Global activation rate (ms)					ECLM-detected cycle length (ms)
150	151.3	147.7				149.5 ± 2.5
170	172.4					172.4
200	200.4	202.8	201.2	200.3	198.8	200.7 ± 1.5
250	248.1	250.6	248.8	249.4		249.2 ± 1.1
300	300.3	301.2	300.8			300.8 ± 0.5
350	348.6					348.6
400	396.8					396.8
500	495.1					495.1

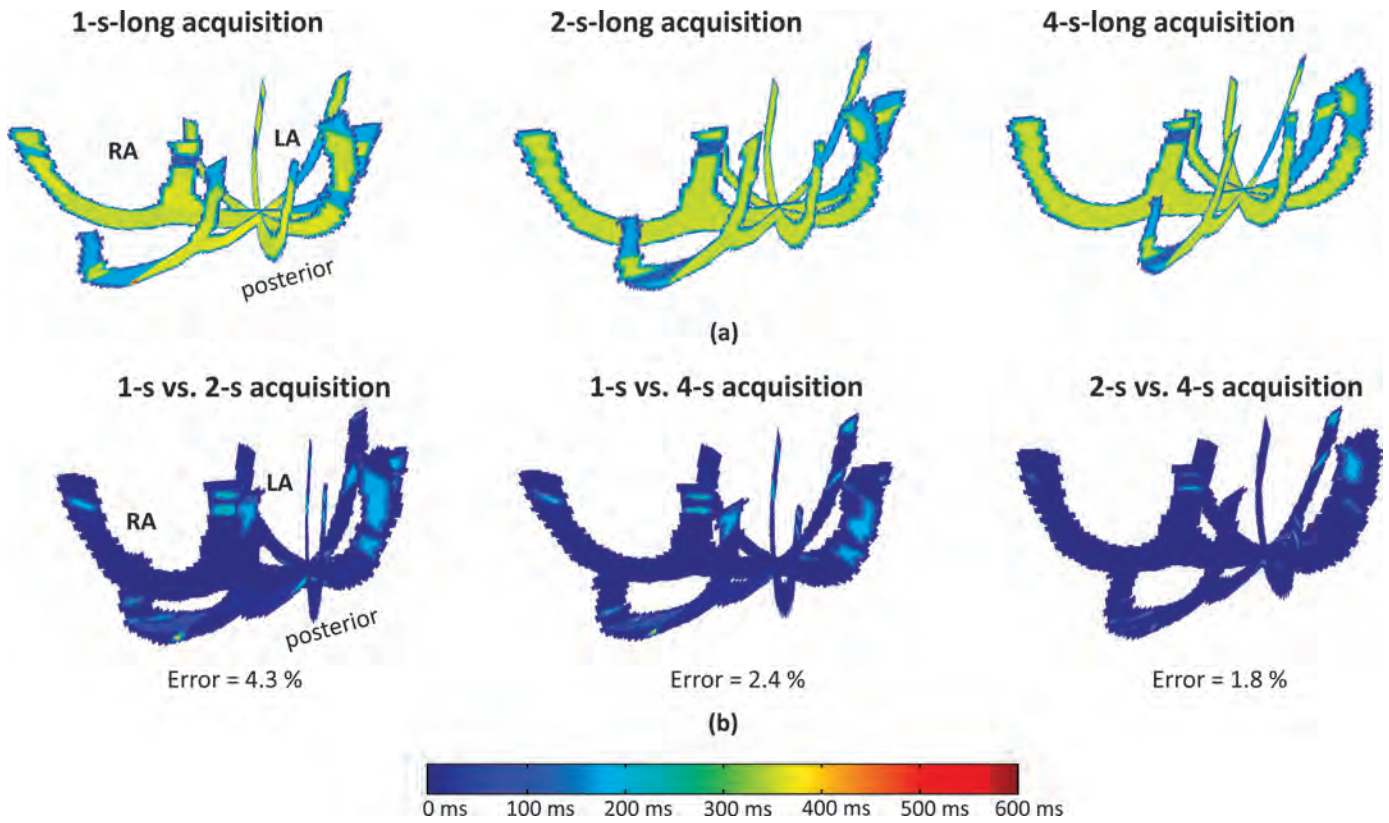


Fig. 5. Effect of signal length on quality of ECLM. ECLM is performed on 1-s, 2-s, and 4-s-long signals sampled at 2000 Hz acquired during pacing at 350 ms. Cycle length maps for each length of acquisition are presented first (a). Then, maps are compared with each other, and absolute difference maps and error values are generated (b). RA: right atrium, LA: left atrium.

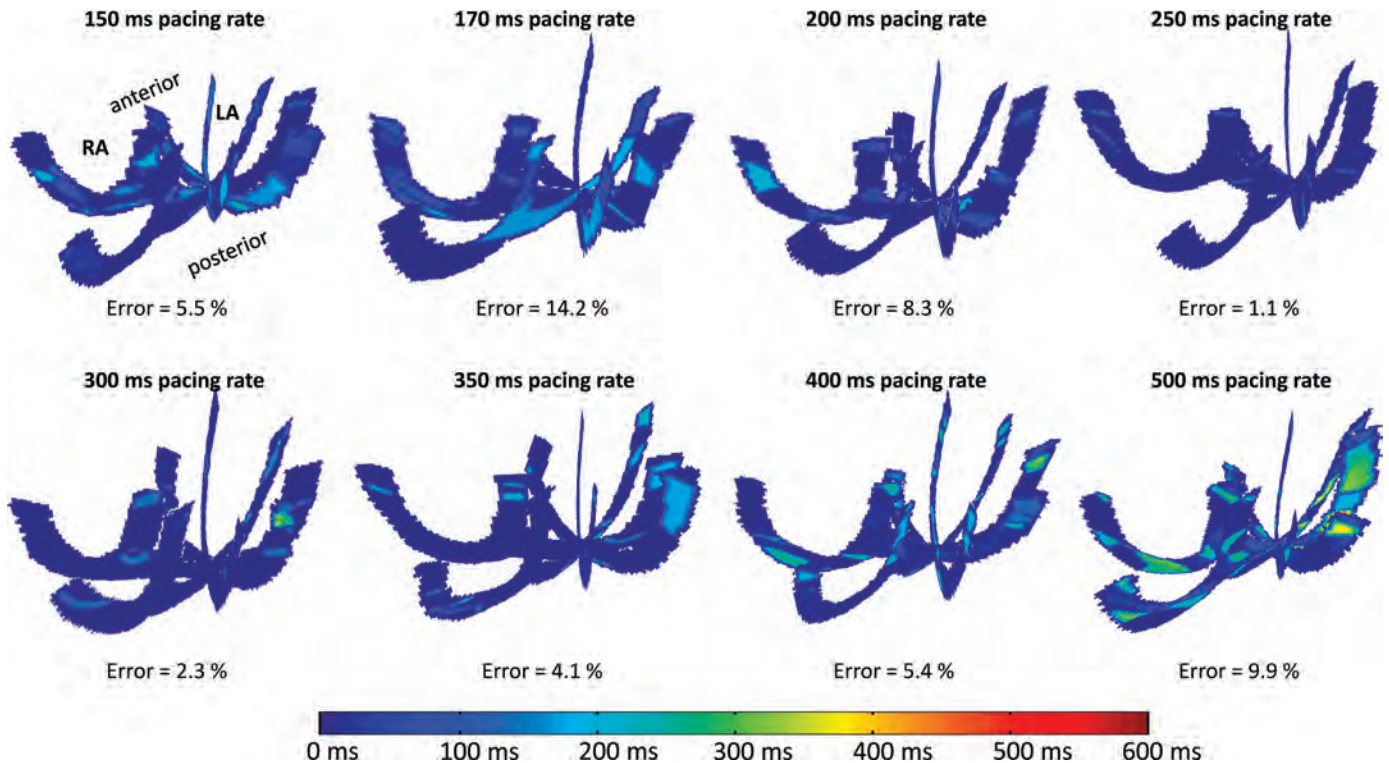


Fig. 6. ECLM reproducibility during pacing. Difference maps as well as the error value between two consecutive acquisitions are presented here for all pacing settings. RA: right atrium, LA: left atrium.

TABLE III. SUMMARY OF ERRORS BETWEEN CONSECUTIVE ACQUISITIONS FOR ALL PACING RATES.

Pacing rates (ms)	150	170	200	250	300	350	400	500
Error (%)	5.5	14.2	8.3	1.1	2.3	4.1	5.4	9.9

the heart seems to activate chaotically on a global scale, whereas, locally, regions of the myocardium activate at various rates, which can then be mapped by ECLM.

Before studying more complex arrhythmias such as AF, it is important to demonstrate that ECLM can correctly detect frequencies of activation, or CL, for more organized arrhythmias such as tachycardia. Figs. 3 and 4 both show that ECLM was capable of detecting the pacing rate at which we paced the atria from the LAA. The pacing rates ranged from 150 to 500 ms, which falls within the range of CL for AF as previously reported [18], [41], [42]. CL maps for each of the pacing rate show that most of the atria is activated at a CL coinciding with the pacing rate. Histograms further confirmed this as the global maximum was detected at a CL corresponding to the pacing rate. We note that at the fastest pacing rates, both the map and the histogram show that some regions in the heart seem to activate more slowly, i.e., at a higher CL, than the expected pacing rate. In the frequency domain, these can correspond to subharmonics of the fundamental frequency of activation corresponding to the pacing rate. Subharmonics may be the result of several phenomena. The first one is that the refractory period of cells in the myocardium might be longer than the rate at which the atria are paced. Indeed, it was reported that the refractory period duration in normal cardiac cells is about 200 to 240 ms but can be reduced to 80 to 85 ms during AF [43]. As such, parts of the atria may not be captured with every pacing beat, resulting in a 2:1 or 3:1 activation pattern in those regions, which then results in regions presenting a higher CL. The second explanation might relate to ventricular contractions. Indeed, at such a fast pacing rate, the ventricle may only be captured every 2 to 3 pacing beats. When they contract, the ventricles affect atrial electromechanical activation via tethering of the cardiac tissue, which may result in lower apparent activation. Although ECLM relies on the frequency content of the incremental strain curve, and as such, only requires a periodic change in the incremental strain curves to derive information about CL, the third phenomenon at play relates to the fact that incremental strain is estimated in the longitudinal direction thus introducing an inherent angle-dependence. Indeed, when the walls of the heart are aligned with the longitudinal direction, incremental strain will alternate between negative values during systole, i.e., contraction, and positive values during diastole, i.e., lengthening. Alternatively, when the wall is perpendicular to the longitudinal direction, incremental strain will alternate between positive values during systole, i.e., thickening of the wall during contraction, and negative values during diastole, i.e., thinning of the wall. However, when the walls are aligned so that the longitudinal direction intersects the myocardium at an angle close to 45°, the magnitude of the changes

in incremental strain will be lower than when the wall is perfectly aligned or perpendicular to the direction of estimation, which may in turn result in corruption by noise and thus inaccurate estimation. At longer pacing rates (250–500 ms), some regions in the atria seem to contract twice as fast as the pacing rate. This could be due to peak hopping: in these regions uncertainties in the strain estimation result in noisy incremental strain curves as well as spectral distortion. These factors may lead to peaks corresponding to harmonics of the fundamental frequency, i.e., the pacing frequency, having higher amplitudes in the frequency domain than the peak corresponding to the pacing frequency. This, in turn, results in incorrect DF estimation and a CL detected that is one-half of the pacing CL.

In Fig. 5, the effect of the length of acquisition on the ECLM performance was studied. The different lengths of acquisition were chosen so that at least two pacing cycles were acquired for all pacing rates. We found that there was virtually no difference between the 1-s, 2-s, and 4-s-long acquisitions both qualitatively and quantitatively, as all three CL maps were qualitatively very similar and the values for the error between the acquisitions were below 5%. The error between the 2-s and 4-s-long acquisitions was the lowest at 1.8%. In the case of the 1-s-long acquisitions, results were slightly noisier although they still correctly detected the global CL at the pacing rate. To obtain the desired frequency resolution when applying the FFT algorithm, we needed to resample the incremental strain curve signals. 2-s and 4-s-long signals were resampled at 40 and 80 Hz, which enabled us to detect frequencies up to 20 and 40 Hz, respectively. Compared with the range of frequencies that is of interest here, i.e., 1.7 to 10 Hz (or cycle lengths from 100 to 600 ms), the sampling was sufficient for accurate mapping. However, when considering the 1-s-long acquisition, the signal was resampled at 20 Hz, which enabled us to detect frequencies up to 10 Hz, which is the upper limit of the range of frequencies of interest, and which may account for slightly less even results when compared with longer acquisition lengths. These results prove that any acquisition length superior to 1 s is sufficient but that one should consider acquisition lengths of at least 2 s for better results. Previous studies in the clinic on DF analysis of electrocardiograms support these findings and have shown that technical considerations for improving the quality of DF analysis include averaging multiple electrocardiograms to improve precision as well as increasing the length of acquisition [9], [18], [44], [45], with 2 s being the minimum for accurate estimation. Furthermore, Habel *et al.* [46] showed that, although point-by-point acquisition of the electrocardiograms is routinely performed in the clinic, simultaneous signal acquisition greatly reduces both the temporal and spatial variability of DF analysis. This strongly emphasizes the advantage of

ECLM in overcoming limitations currently attributed to available techniques in the clinic by enabling simultaneous, whole-atria acquisition.

Finally, in Fig. 6 we showed that ECLM was highly reproducible across the whole range of pacing rates that was considered, with results for CL in the range of 250 to 350 ms being the most reproducible. In this study, we considered a model of arrhythmia which produced organized rhythms, as opposed to chaotic rhythms such as is the case during AF. Indeed, by pacing the atria at pre-determined pacing rates, we obtained a canine atrial tachycardia model where most of the myocardium is expected to activate at a similar rate. A limitation of the current method is that when considering more complex arrhythmias such as AF, the global activation rate is not well adapted due to the chaotic nature of activation during AF resulting in regions activating at different rates across the atria [11], [15] and due to the presence of drivers that may not be spatio-temporally stable (including meandering re-entry circuits and rotors) [47], [48]. However, because ECLM enables simultaneous mapping of the whole atria in a single heart-beat, we believe that we may use ECLM for the study of local activation rate in a neighborhood of points within the myocardium. This in turn may facilitate the study of AF drivers and ultimately may help guide or shorten the duration of the treatment of such arrhythmias. Using ECLM for the study of more complex arrhythmias, such as AF, is the focus of ongoing studies within our group.

V. CONCLUSION

In this study, we introduced a new echocardiography-based mapping method called ECLM, which estimates the CL of the electromechanical activation rate within the heart in a single acquisition. ECLM was validated for a range of pacing rates corresponding to activation rates previously reported for nonperiodic arrhythmias such as AF. ECLM was shown to be repeatable and feasible on short acquisitions of the order of a couple of seconds. These findings indicate that ECLM may be a useful planning and follow-up tool for the characterization of atrial arrhythmias such as AF or atrial flutter by noninvasively and transthoracically providing insights into the underlying diseases, with the long-term goal of reducing the duration while increasing the success rate of catheter ablation procedures.

REFERENCES

- [1] V. Fuster, L. E. Rydén, D. S. Cannom, H. J. Crijns, A. B. Curtis, K. A. Ellenbogen, J. L. Halperin, J.-Y. L. Heuzey, G. N. Kay, J. E. Lowe, S. B. Olsson, E. N. Prystowsky, J. L. Tamargo, S. Wann, S. C. Smith, A. K. Jacobs, C. D. Adams, J. L. Anderson, E. M. Antman, J. L. Halperin, S. A. Hunt, R. Nishimura, J. P. Ornato, R. L. Page, B. Riegel, S. G. Priori, J.-J. Blanc, A. Budaj, A. J. Camm, V. Dean, J. W. Deckers, C. Despres, K. Dickstein, J. Lekakis, K. McGregor, M. Metra, J. Morais, A. Osterspey, J. L. Tamargo, and J. L. Zamorano, "ACC/AHA/ESC 2006 Guidelines for the management of patients with atrial fibrillation—Executive Summary A Report of the American College of Cardiology/American Heart Association Task Force on Practice Guidelines and the European Society of Cardiology Committee for Practice Guidelines (Writing Committee to Revise the 2001 Guidelines for the management of patients with atrial fibrillation): Developed in collaboration with the European Heart Rhythm Association and the Heart Rhythm Society," *Circulation*, vol. 114, no. 7, pp. e257–e354, Aug. 2006.
- [2] L. S. Jenkins, M. Brodsky, E. Schron, M. Chung, and T. Rocco JrE. Lader, M. Constantine, R. Sheppard, D. Holmes, D. Mateski, L. Floden, M. Prasad, H. L. Greene, and L. Shemanski "Quality of life in atrial fibrillation: The Atrial Fibrillation Follow-up Investigation of Rhythm Management (AFFIRM) study," *Am. Heart J.*, vol. 149, no. 1, pp. 112–120, Jan. 2005.
- [3] E. J. Benjamin, P. A. Wolf, R. B. D'Agostino, H. Silbershatz, W. B. Kannel, and D. Levy, "Impact of atrial fibrillation on the risk of death: The Framingham Heart Study," *Circulation*, vol. 98, no. 10, pp. 946–952, Sep. 1998.
- [4] S. S. Chugh, R. Havmoeller, K. Narayanan, D. Singh, M. Rienstra, E. J. Benjamin, R. F. Gillum, Y.-H. Kim, J. H. McAnulty, Z.-J. Zheng, M. H. Forouzanfar, M. Naghavi, G. A. Mensah, M. Ezzati, and C. J. L. Murray, "Worldwide epidemiology of atrial fibrillation: A global burden of disease 2010 study," *Circulation*, art. no. CIRCULATIONAHA.113.005119, Dec. 2013.
- [5] D. R. Van Wagoner, J. P. Piccini, C. M. Albert, M. E. Anderson, E. J. Benjamin, B. Brundel, R. M. Califf, H. Calkins, P.-S. Chen, N. Chiamvimonvat, D. Darbar, L. L. Eckhardt, P. T. Ellinor, D. V. Exner, R. I. Fogel, A. M. Gillis, J. Healey, S. H. Hohnloser, H. Kannel, D. A. Lathrop, G. Y. H. Lip, R. Mehra, S. M. Narayan, J. Olgin, D. Packer, N. S. Peters, D. M. Roden, H. M. Ross, R. Sheldon, and X. H. T. Wehrens, "Progress toward the prevention and treatment of atrial fibrillation: A summary of the Heart Rhythm Society Research Forum on the Treatment and Prevention of Atrial Fibrillation, Washington, DC, December 9–10, 2013," *Heart Rhythm*, vol. 12, no. 1, pp. e5–e29, Jan. 2015.
- [6] H. Calkins, K. H. Kuck, R. Cappato, J. Brugada, A. J. Camm, S.-A. Chen, H. J. G. Crijns, J. Ralph, J. Damiano, D. W. Davies, J. DiMarco, J. Edgerton, K. Ellenbogen, M. D. Ezekowitz, D. E. Haines, M. Haissaguerre, G. Hindricks, Y. Iesaka, W. Jackman, J. Jalife, P. Jais, J. Kalman, D. Keane, Y.-H. Kim, P. Kirchhof, G. Klein, H. Kottkamp, K. Kumagai, B. D. Lindsay, M. Mansour, F. E. Marchlinski, P. M. McCarthy, J. L. Mont, F. Morady, K. Nademanee, H. Nakagawa, and A. Natale, SD. L. Nattel, C. Packer, E. Pappone, A. Prystowsky, V. Raviele, J. N. Reddy, R. J. Ruskin, H.-M. Shemin, D. Tsao, H. Wilber, K. H. Calkins, R. Kuck, S.-A. Cappato, E. N. Chen, K. H. Prystowsky, A. Kuck, D. E. Natale, F. E. Haines, H. Marchlinski, D. W. Calkins, B. D. Davies, J. Lindsay, D. L. Ralph Damiano, J. Packer, A. J. Brugada, H. J. G. Camm, J. Crijns, J. DiMarco, K. Edgerton, M. D. Ellenbogen, M. Ezekowitz, G. Haissaguerre, Y. Hindricks, W. M. Iesaka, P. Jackman, J. Jais, J. Jalife, D. Kalman, Y.-H. Keane, P. Kim, G. Kirchhof, H. Klein, K. Kottkamp, M. Kumagai, F. Mansour, P. Marchlinski, J. L. McCarthy, F. Mont, K. Morady, H. Nademanee, S. Nakagawa, C. Nattel, A. Pappone, V. Raviele, J. N. Reddy, R. J. Ruskin, H.-M. Shemin, D. Tsao, N. Wilber, J. Ad, A. M. Cummings, H. Gillinov, C. Heidebuchel, G. January, S. Lip, M. Markowitz, I. E. Nair, H.-N. Ovsyshcher, T. Pak, D. Tsuchiya, T. W. Shah, Siong, and P. E. Vardas, "2012 HRS/EHRA/ECAS Expert consensus statement on catheter and surgical ablation of atrial fibrillation: Recommendations for patient selection, procedural techniques, patient management and follow-up, definitions, endpoints, and research trial design," *Europace*, vol. 14, no. 4, pp. 528–606, Feb. 2012.
- [7] R. Hatala, C. Weiss, D. H. Koschyk, J. Siebels, R. Cappato, and K.-H. Kuck, "Radio-frequency catheter ablation of left atrial tachycardia originating within the pulmonary vein in a patient with dextrocardia," *Pacing Clin. Electrophysiol.*, vol. 19, no. 6, pp. 999–1002, 1996.
- [8] L.-F. Hsu, P. Jais, P. Sanders, S. Garrigue, M. Hocini, F. Sacher, Y. Takahashi, M. Rotter, J.-L. Pasquie, C. Scavée, P. Bordachar, J. Clémenty, and M. Haissaguerre, "Catheter ablation for atrial fibrillation in congestive heart failure," *N. Engl. J. Med.*, vol. 351, no. 23, pp. 2373–2383, Dec. 2004.
- [9] M. K. Stiles, A. G. Brooks, B. John, L. Wilson, P. Kuklik, H. Dimitri, D. H. Lau, R. L. Roberts-Thomson, L. Mackenzie, and S. Wiloughby, "The effect of electrogram duration on quantification of complex fractionated atrial electrograms and dominant frequency," *J. Cardiovasc. Electrophysiol.*, vol. 19, no. 3, pp. 252–258, 2008.

- [10] R. J. Schilling, N. S. Peters, and D. W. Davies, "Simultaneous endocardial mapping in the human left ventricle using a noncontact catheter comparison of contact and reconstructed electrograms during sinus rhythm," *Circulation*, vol. 98, no. 9, pp. 887–898, Sep. 1998.
- [11] S. Lazar, S. Dixit, F. E. Marchlinski, D. J. Callans, and E. P. Gerstenfeld, "Presence of left-to-right atrial frequency gradient in paroxysmal but not persistent atrial fibrillation in humans," *Circulation*, vol. 110, no. 20, pp. 3181–3186, 2004.
- [12] J. Sahadevan, K. Ryu, L. Peltz, C. M. Khrestian, R. W. Stewart, A. H. Markowitz, and A. L. Waldo, "Epicardial mapping of chronic atrial fibrillation in patients preliminary observations," *Circulation*, vol. 110, no. 21, pp. 3293–3299, 2004.
- [13] P. Sanders, O. Berenfeld, M. Hocini, P. Jais, R. Vaidyanathan, L.-F. Hsu, S. Garrigue, Y. Takahashi, M. Rotter, and F. Sacher, "Spectral analysis identifies sites of high-frequency activity maintaining atrial fibrillation in humans," *Circulation*, vol. 112, no. 6, pp. 789–797, 2005.
- [14] T. H. Everett, E. E. Wilson, S. Verheule, J. M. Guerra, S. Foreman, and J. E. Olgin, "Structural atrial remodeling alters the substrate and spatiotemporal organization of atrial fibrillation: A comparison in canine models of structural and electrical atrial remodeling," *Am. J. Physiol. Heart Circ. Physiol.*, vol. 291, no. 6, pp. H2911–H2923, Dec. 2006.
- [15] S. R. Dibs, J. Ng, R. Arora, R. S. Passman, A. H. Kadish, and J. J. Goldberger, "Spatiotemporal characterization of atrial activation in persistent human atrial fibrillation: Multisite electrogram analysis and surface electrocardiographic correlations—A pilot study," *Heart Rhythm*, vol. 5, no. 5, pp. 686–693, May 2008.
- [16] R. Mandapati, A. Skanes, J. Chen, O. Berenfeld, and J. Jalife, "Stable microreentrant sources as a mechanism of atrial fibrillation in the isolated sheep heart," *Circulation*, vol. 101, no. 2, pp. 194–199, Jan. 2000.
- [17] S. Lazar, S. Dixit, D. J. Callans, D. Lin, F. E. Marchlinski, and E. P. Gerstenfeld, "Effect of pulmonary vein isolation on the left-to-right atrial dominant frequency gradient in human atrial fibrillation," *Heart Rhythm*, vol. 3, no. 8, pp. 889–895, 2006.
- [18] J. Ng and J. J. Goldberger, "Understanding and interpreting dominant frequency analysis of AF electrograms," *J. Cardiovasc. Electrophysiol.*, vol. 18, no. 6, pp. 680–685, 2007.
- [19] Y.-J. Lin, H.-M. Tsao, S.-L. Chang, L.-W. Lo, Y.-F. Hu, C.-J. Chang, W.-C. Tsai, K. Suenari, S.-Y. Huang, and H.-Y. Chang, "Role of high dominant frequency sites in nonparoxysmal atrial fibrillation patients: Insights from high-density frequency and fractionation mapping," *Heart Rhythm*, vol. 7, no. 9, pp. 1255–1262, 2010.
- [20] Y. Takahashi, P. Sanders, P. Jais, M. Hocini, R. Dubois, M. Rotter, T. Rostock, C. J. Nalliah, F. Sacher, and J. Clémenty, "Organization of frequency spectra of atrial fibrillation: Relevance to radiofrequency catheter ablation," *J. Cardiovasc. Electrophysiol.*, vol. 17, no. 4, pp. 382–388, 2006.
- [21] Y.-J. Lin, C.-T. Tai, T. Kao, H.-W. Tso, S. Higa, H.-M. Tsao, S.-L. Chang, M.-H. Hsieh, and S.-A. Chen, "Frequency analysis in different types of paroxysmal atrial fibrillation," *J. Am. Coll. Cardiol.*, vol. 47, no. 7, pp. 1401–1407, 2006.
- [22] J. L. Wells, W. A. MacLean, T. N. James, and A. L. Waldo, "Characterization of atrial flutter. Studies in man after open heart surgery using fixed atrial electrodes," *Circulation*, vol. 60, no. 3, pp. 665–673, Sep. 1979.
- [23] M. Pernot, K. Fujikura, S. D. Fung-Kee-Fung, and E. E. Konofagou, "ECG-gated, mechanical and electromechanical wave imaging of cardiovascular tissues in vivo," *Ultrasound Med. Biol.*, vol. 33, no. 7, pp. 1075–1085, 2007.
- [24] J. Provost, W.-N. Lee, K. Fujikura, and E. E. Konofagou, "Imaging the electromechanical activity of the heart in vivo," *Proc. Natl. Acad. Sci. USA*, vol. 108, no. 21, pp. 8565–8570, May 2011.
- [25] J. Provost, S. Thiébaud, J. Luo, and E. E. Konofagou, "Single-heart-beat electromechanical wave imaging with optimal strain estimation using temporally unequipped acquisition sequences," *Phys. Med. Biol.*, vol. 57, no. 4, pp. 1095–1112, Feb. 2012.
- [26] A. Costet, J. Provost, A. Gambhir, Y. Bobkov, P. Danilo Jr., G. J. J. Boink, M. R. Rosen, and E. E. Konofagou, "Electromechanical wave imaging of biologically and electrically paced canine hearts in vivo," *Ultrasound Med. Biol.*, vol. 40, no. 1, pp. 177–187, Jan. 2014.
- [27] J. Luo and E. Konofagou, "A fast normalized cross-correlation calculation method for motion estimation," *IEEE Trans. Ultrason. Ferroelectr. Freq. Control*, vol. 57, no. 6, pp. 1347–1357, Jun. 2010.
- [28] F. Kallel and J. Ophir, "A least-squares strain estimator for elastography," *Ultrason. Imaging*, vol. 19, no. 3, pp. 195–208, 1997.
- [29] H. Chen, T. Varghese, P. S. Rahko, and J. A. Zagzebski, "Ultrasound frame rate requirements for cardiac elastography: Experimental and in vivo results," *Ultrasonics*, vol. 49, no. 1, pp. 98–111, Jan. 2009.
- [30] J. Provost, V. T.-H. Nguyen, D. Legrand, S. Okrasinski, A. Costet, A. Gambhir, H. Garan, and E. E. Konofagou, "Electromechanical wave imaging for arrhythmias," *Phys. Med. Biol.*, vol. 56, no. 22, pp. L1–L11, Nov. 2011.
- [31] J. Provost, A. Gambhir, J. Vest, H. Garan, and E. E. Konofagou, "A clinical feasibility study of atrial and ventricular electromechanical wave imaging," *Heart Rhythm*, vol. 10, no. 6, pp. 856–862, Jun. 2013.
- [32] J. Luo and E. E. Konofagou, "High-frame rate, full-view myocardial elastography with automated contour tracking in murine left ventricles in vivo," *IEEE Trans. Ultrason. Ferroelectr. Freq. Control*, vol. 55, no. 1, pp. 240–248, Jan. 2008.
- [33] H. Chen, H. Shi, and T. Varghese, "Improvement of elastographic displacement estimation using a two-step cross-correlation method," *Ultrasound Med. Biol.*, vol. 33, no. 1, pp. 48–56, 2007.
- [34] W.-N. Lee, Z. Qian, C. L. Tosti, T. R. Brown, D. N. Metaxas, and E. E. Konofagou, "Preliminary validation of angle-independent myocardial elastography using MR tagging in a clinical setting," *Ultrasound Med. Biol.*, vol. 34, no. 12, pp. 1980–1997, 2008.
- [35] W. F. Walker and G. E. Trahey, "A fundamental limit on the performance of correlation based phase correction and flow estimation techniques," *IEEE Trans. Ultrason. Ferroelectr. Freq. Control*, vol. 41, no. 5, pp. 644–654, 1994.
- [36] W. F. Walker and G. E. Trahey, "A fundamental limit on delay estimation using partially correlated speckle signals," *IEEE Trans. Ultrason. Ferroelectr. Freq. Control*, vol. 42, no. 2, pp. 301–308, 1995.
- [37] T. Varghese and J. Ophir, "A theoretical framework for performance characterization of elastography: The strain filter," *IEEE Trans. Ultrason. Ferroelectr. Freq. Control*, vol. 44, no. 1, pp. 164–172, 1997.
- [38] R. Righetti, J. Ophir, and P. Ktonas, "Axial resolution in elastography," *Ultrasound Med. Biol.*, vol. 28, no. 1, pp. 101–113, Jan. 2002.
- [39] D. M. Bers, "Cardiac excitation-contraction coupling," *Nature*, vol. 415, no. 6868, pp. 198–205, Jan. 2002.
- [40] J. M. Cordeiro, L. Greene, C. Heilmann, D. Antzelevitch, and C. Antzelevitch, "Transmural heterogeneity of calcium activity and mechanical function in the canine left ventricle," *Am. J. Physiol. Heart Circ. Physiol.*, vol. 286, no. 4, pp. H1471–H1479, Apr. 2004.
- [41] A. E. Buxton, H. L. Waxman, F. E. Marchlinski, and M. E. Josephson, "Atrial conduction: Effects of extrastimuli with and without atrial dysrhythmias," *Am. J. Cardiol.*, vol. 54, no. 7, pp. 755–761, Oct. 1984.
- [42] M. Haïssaguerre, P. Sanders, M. Hocini, L.-F. Hsu, D. C. Shah, C. Scavée, Y. Takahashi, M. Rotter, J.-L. Pasquié, S. Garrigue, J. Clémenty, and P. Jais, "Changes in atrial fibrillation cycle length and inducibility during catheter ablation and their relation to outcome," *Circulation*, vol. 109, no. 24, pp. 3007–3013, Jun. 2004.
- [43] V. N. Biktashev, "Control of re-entrant vortices by electrical stimulation," in *Computational Biology of the Heart*, 1st ed., A. V. Panfilov and A. V. Holden, Eds. Chichester, UK: Wiley, 1997, pp. 137–170.
- [44] S. M. Narayan, D. E. Krummen, A. M. Kahn, P. L. Karasik, and M. R. Franz, "Evaluating fluctuations in human atrial fibrillatory cycle length using monophasic action potentials," *Pacing Clin. Electrophysiol.*, vol. 29, no. 11, pp. 1209–1218, 2006.
- [45] A. B. Biviano, J. Coromilas, E. J. Ciaccio, W. Whang, K. Hickey, and H. Garan, "Frequency domain and time complex analyses manifest low correlation and temporal variability when calculating activation rates in atrial fibrillation patients," *Pacing Clin. Electrophysiol.*, vol. 34, no. 5, pp. 540–548, 2011.
- [46] N. Habel, P. Znojkwicz, N. Thompson, J. G. Müller, B. Mason, J. Calame, S. Calame, S. Sharma, G. Mirchandani, and D. Janks, "The temporal variability of dominant frequency and complex fractionated atrial electrograms constrains the validity of sequential mapping in human atrial fibrillation," *Heart Rhythm*, vol. 7, no. 5, pp. 586–593, 2010.
- [47] M. Haïssaguerre, M. Hocini, A. Denis, A. J. Shah, Y. Komatsu, S. Yamashita, M. Daly, S. Amraoui, S. Zellerhoff, M.-Q. Picat, A. Quotb, L. Jesel, H. Lim, S. Ploux, P. Bordachar, G. Attuel, V. Meillet, P. Ritter, N. Derval, F. Sacher, O. Bernus, H. Cochet, P. Jais, and R. Dubois, "Driver domains in persistent atrial fibrillation," *Circulation*, vol. 130, no. 7, pp. 530–538, Aug. 2014.

- [48] M. Rodrigo, M. S. Guillem, A. M. Climent, J. Pedrón-Torrecilla, A. Liberós, J. Millet, F. Fernández-Avilés, F. Atienza, and O. Berenfeld, "Body surface localization of left and right atrial high-frequency rotors in atrial fibrillation patients: A clinical-computational study," *Heart Rhythm*, vol. 11, no. 9, pp. 1584–1591, Sep. 2014.



Alexandre Costet received two M.S. degrees, one in electrical engineering from Supélec, Paris, France, and the other in biomedical engineering from Imperial College, London, UK, in 2008. His work as a graduate student at Imperial College focused on image processing techniques for ultrasound elasticity imaging and applications to breast cancer detection and characterization. He is currently a Ph.D. candidate in the Department of Biomedical Engineering at Columbia University. His current research interests include echocardiography and elasticity imaging of the heart using electromechanical wave imaging, in particular when relating to atrial arrhythmia such as atrial tachycardia, flutter, and fibrillation.

diography and elasticity imaging of the heart using electromechanical wave imaging, in particular when relating to atrial arrhythmia such as atrial tachycardia, flutter, and fibrillation.



Ethan Bunting was born in Wilmington, Delaware, USA, and completed his undergraduate studies at the University of Virginia, graduating in May 2011 with a B.S. degree in biomedical engineering. He conducted his undergraduate research in a cardiac mechanics lab, where he focused on developing an imaging technique that could be used to accurately map the lead locations in patients with bi-ventricular pacemakers. In September 2011, Ethan enrolled in the M.S./Ph.D. program in the Department of Biomedical

Engineering at Columbia University. His current research interests include novel imaging techniques used to examine the electrical and mechanical activity of the heart, especially in diagnostic and clinical applications.



Julien Grondin was born in June 1983 in Saint-Denis, Reunion Island (France). He received his M.S. degree from University of Paris VII in 2007 and his Ph.D. degree from the University of Paris VI in 2010. His main focus was on ultrasonic characterization of bone properties. He joined the Ultrasound and Elasticity Imaging Laboratory as a postdoctoral research scientist in 2011 and is currently an associate research scientist in the Department of Biomedical Engineering at Columbia University, New York. His research interests include cardiac ultrasound imaging, myocardial elastography, and HIFU ablation monitoring.

include cardiac ultrasound imaging, myocardial elastography, and HIFU ablation monitoring.



Alok Gambhir, M.D., received his medical degree from State University of New York (SUNY) at Stony Brook School of Medicine and completed his residency in internal medicine at The Mount Sinai Hospital in New York. He received M.A. and Ph.D. degrees in physics from SUNY at Stony Brook in New York and an undergraduate degree from Birmingham Southern in Alabama. He completed an advanced fellowship in cardiac electrophysiology at Columbia University Medical Center in New York, where he was previously a

cardiology fellow, as well as a biomedical engineering research associate. He was also a cardiac electrophysiology fellow at NYU Langone Medical Center. Dr. Gambhir is now board-eligible in internal medicine, cardiovascular disease, and clinical cardiac electrophysiology at the Heart Center of Northeast Georgia Medical Center. His research and clinic interests include the study and treatment on complex arrhythmias; in particular, Dr. Gambhir has extensive experience with more complicated ventricular tachycardia and atrial fibrillation ablations. In addition to his clinical experience, he has published extensively in this area of expertise. Dr. Gambhir also has experience with the LARIAT procedure—treatment for the left atrial appendage, and a special interest in cardiogenetics and congenital heart disease.



Elisa Konofagou is an Associate Professor of biomedical engineering and radiology and Director of the Ultrasound and Elasticity Imaging Laboratory at Columbia University in New York, NY. Her main interests are in the development of novel elasticity imaging techniques and therapeutic ultrasound methods, and more notably, myocardial elastography, electromechanical and pulse wave imaging, harmonic motion imaging, and focused ultrasound therapy and drug delivery in the brain, with several clinical collaborations in the Colum-

bia Presbyterian Medical Center and elsewhere. Prof. Konofagou is a member of the IEEE; the IEEE Engineering in Medicine and Biology Society; the IEEE Ultrasonics, Ferroelectrics, and Frequency Control Society; the Acoustical Society of America; and the American Institute of Ultrasound in Medicine. Prof. Konofagou is also a technical committee member of the Acoustical Society of America, the International Society of Therapeutic Ultrasound, the IEEE Engineering in Medicine and Biology Conference (EMBC), the IEEE International Ultrasonics Symposium, and the American Association of Physicists in Medicine (AAPM), and is a former technical standards committee member of the American Institute of Ultrasound in Medicine. She serves as an Associate Editor for the *Medical Physics* journal, is on the Editorial Board for *Ultrasound In Medicine and Biology*, and is recipient of awards from the American Heart Association, the Acoustical Society of America, the American Institute of Ultrasound in Medicine, the Wallace H. Coulter foundation, the National Institutes of Health, the National Science Foundation, and the Radiological Society of North America.